Distribution of suspended particulate matter at the equatorial transect in the Atlantic Ocean

Vadim Sivkov[1,2] and Ekaterina Bubnova[1,2]

[1]Shirshov Institute of Oceanology, Russian Academy of Sciences, 36, Nahimovskiy prospekt, Moscow, Russia, 117997
[2]Immanuel Kant Baltic Federal University, Kaliningrad, 14, A. Nevskogo str., Kaliningrad, Russia, 236016

Correspondence: Ekaterina Bubnova (bubnova.kat@gmail.com)

Abstract. Studied oceanographic transect across the Equatorial Atlantic is considered as "screenshot" of suspended particulate matter distribution against a hydrographical background. The area of abnormal high suspended matter volume concentrations was found above the Sierra Leone Rise from top to bottom (eastern part of the transect). The suggested explanation for the anomaly is based on the ballast hypothesis whereby solid particles are incorporated as ballast into suspended biogenic aggre-
5 gates, leading to increased velocities of sinking. This process is located within the Northwest African upwelling area, since the plankton exposed to the Saharan dust abundance form a significant number of aggregates lately transported equatorward via Canary Current. The intermediate nepheloid layer associated with the Deep Western Boundary Current was recorded from the American Slope at the 3200–3700 m to the depth of 4300 m above the Para Abyssal Plain. Antarctic Bottom Water enriched in suspended matter was found mostly in the troughs at 40–41° W. It was detached from the bottom, coinciding with the core
10 of the flow due to the bottom rise ("dam") located up-stream. The grain size of particles was in accordance with polymodal distribution — the 2–4 μm and the 8–13 μm modes. The registered rise in percentage of the 7–21 μm-sized particles suggests the presence of the well-known coarse mode (20–60 μm) formed by aggregation of transparent exopolymer particles (mucus).

1   Introduction

Numerous studies have focused on characterizing the suspended particulate matter (SPM) during the past half a century due to
15 the fact of its importance. Modern understanding of the basic patterns of the SPM distribution in the ocean had emerged by the end of the 1980s (Chester, 1990). Therefore, the oceanic SPM spread may be depicted as a three-layer structure with following layers (a) a surface water, (b) a clear water minimum, and (c) a deep-water (Biscaye and Eittreim, 1977; Chester, 1990). It was also indicated that the distribution of the SPM in oceans shows basically the interaction between the bottom sediments and abyssal waters movement, so SPM-rich benthic nepheloid layers (BNLs) coincide with pathways of the western boundary
20 currents (Biscaye and Eittreim, 1977). There are also strong intermediate nepheloid layers (INLs) in the clear water minimum layer in some regions (Thorpe and White, 1988).

The Geochemical Ocean Transects study (GEOSECS) has introduced a first description of the suspended particles distribution in the ocean, taking into account mostly SPM collected via filtration (Craig and Turekian, 1976). The three-layer model of the SMP concentration distribution was also successively described in (Brewer et al., 1976) at a transect through the western

25 Atlantic Ocean: high concentrations were found in surface and in rapidly moving bottom waters, while low concentrations were observed in the mid-water regions of the sub-tropical gyres.

The SPM plays a crucial role in both regulation the sea water composition and material transport throughout the entire water column, experiencing various processes (e.g. dissolution, decomposition, disaggregation, aggregation, etc.) (Gardner et al., 1985a). It was shown (McCave, 1975) that the SPM sizes follow a hyperbolic distribution with increase of the fine particles

30 abundance, whereby most of the particle flux to the bottom lies in the coarser size classes.

Sinking particles may remove the dissolved trace elements from solution (Lal, 1977) and transport them to bottom sediments. The extent to which the behavior of dissolved trace elements is dominated by suspended solids was referred as the great particle conspiracy (Turekian, 1977).

The summary in (Jeandel et al., 2015) shows that fine particles (<53 μm) represent the vast majority of particles in the ocean.

35 According to (Sheldon et al., 1972) the size spectrum of small particles varies predictably both geographically and with depth. A linkage of strong BNLs and bentic storms with upper ocean dynamic was described in (Gardner et al., 2018). Yet the full characterization of fine SPM distribution and composition in the ocean remains studied insufficiently due to the high research costs. Thus, the transect research of the fine SPM distribution are still demanded.

The Equatorial Atlantic is the area of increased oceanographic interest owing to the central position on the global circulation

40 map. The aim of this study was to explain the distribution of fine SPM and size spectra at the transatlantic oceanographic transect in the equatorial zone of the Atlantic Ocean (Ioffe-2000 transect). The hydrophysical and hydrochemical data (background for the SPM distribution) have been published in sufficient detail (Sokov et al., 2002; Sarafanov et al., 2007). The SPM data, on the contrary, have been published only briefly (Sivkov et al., 2001) due to the significant differences between the obtained data and the currently accepted conception on this matter (Biscaye and Eittreim, 1977). So far, the ideas have been formed to

45 explain the features of the SPM distribution obtained on the transect.

2   Materials and Methods

A sublatitudinal transect (13–28 July 2000) between the continental slopes of Guinea and Brazil with closely spaced 61 stations was performed during the 8th cruise of the R/V *Akademik Ioffe* (Fig. 1). Additional surface samples of SPM were taken in the Northwest African upwelling zone (Cap Blanc area) just before the transect conduction (10–11 July 2000). Sampling at the

50 Ioffe-2000 transect was carried out using the hydrological complex, equiped with 5 L Niskin bottles, while the additional surface sampling was carried out with a use of plastic bucket.

The SPM volume concentration and particle size distribution were determined by the conductometric method via the Coulter counter (Z_{bi} model) for 407 samples from the Ioffe-2000 transect and 13 samples from the Cap Blanc area (Supplement 1). The Coulter counter calibration was carried out using Coulter Electronics standard methodology using 5.96 μm diameter latex par-

55 ticles. The 70 μm aperture was used, which ensured counting of particles in the size range of 1.8–20.7 μm. Volume suspended solids concentration and size distribution were calculated based on the assumption of particle sphericity. The distributions of temperature, salinity, dissolved oxygen and silicates on the transect (Sokov et al., 2002; Sarafanov et al., 2007) were used in
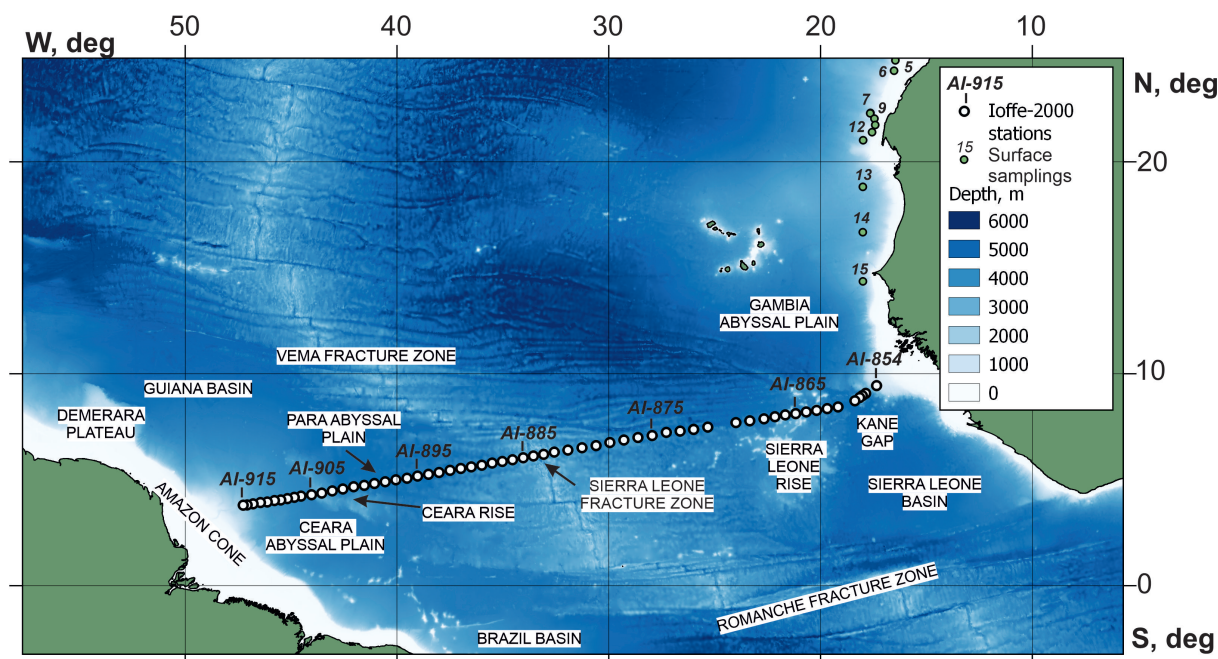
Figure 1. The Ioffe-2000 transect position in the study area (station numbers, every 10 stations). Bottom topography taken according to (GEBCO Bathymetric Compilation Group, 2020).

relation to the SPM data. The temperature and salinity data were recorded via an Neil Brown Mark-III CTD profile (accuracy of measurements was 0.002°C for temperature, 0.002 psu for salinity). The temperature accuracy was determined via precruise

60 and postcruise laboratory calibrations, and the salinity accuracy was calculated by comparison with the bottle data. Water samples for additional salinity measurement and silicate concentrations were obtained using the hydrological complex mentioned above at every station. The silicate concentrations were determined according to the standard method (Mullin and Riley, 1955) (with the accuracy better than 0.2 µmol kg^{-1}) (Sokov et al., 2002; Sarafanov et al., 2007).

3 Hydrographical settings

65 ### 3.1 Upper ocean

The upper levels of the Equatorial Atlantic water structure are dominated by the presence of large-scale westward currents and eastward countercurrents (Fig. 2A). The northern part of the studied region includes an eastward flowing North Equatorial Countercurrent (NECC) at depths 0–100 m and the North Equatorial Undercurrent (NEUC) at depths between 100 m and 300 m (Wilson et al., 1994; Bischof et al., 2003), a westward flowing North Equatorial Current (NEC) and South Equatorial Current

70 (SEC) (Bourlès et al., 1999).
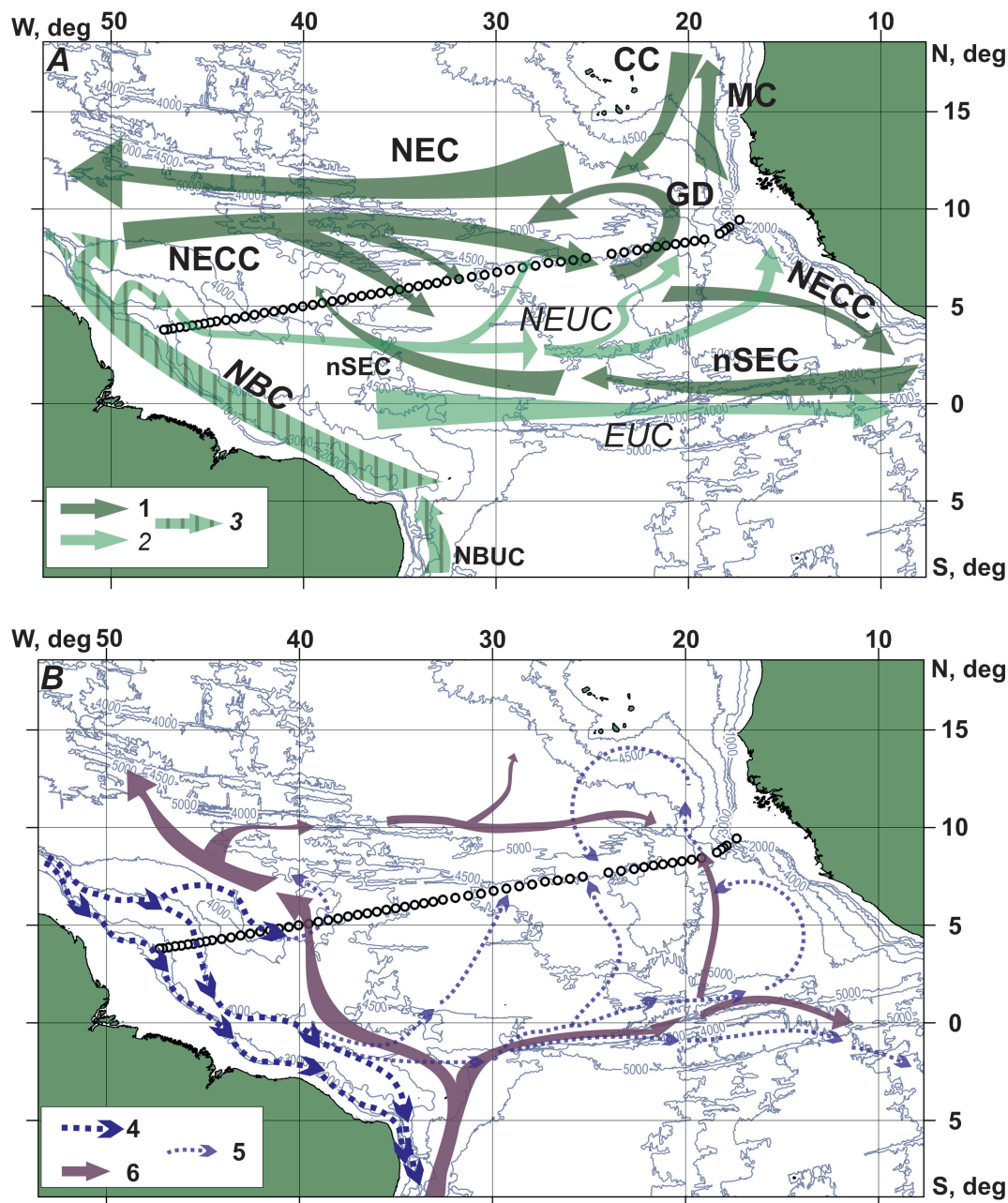
Figure 2. Generalized circulation schematics within the study area: surface and subsurface layers (A) and intermediate, deep, and bottom layers (B), where 1 — surface currents, 2 — subsurface currents, 3 — deep surface currents, 4 — the DWBC cores, 5 — schematic DWBC recirculation, 6 — AABW. The references and current abbreviations are explained in the text. Isobaths every 500 m.

The North Brazil Current (NBC) is a major western boundary current in the Atlantic Ocean, that transports water to the north across the equator within the upper 300 m (Johns et al., 1998; Bischof et al., 2003). The NBC starts as a northern branch of water originating from the SEC as it bifurcates nearby the Brazilian continental shelf at about 10° S, which turns the SEC to the north, and then it merges with the North Brazil Undercurrent (NBUC). The NBC passes the equator, caring Tropical Surface Water (TSW, mixed surface layer) at the 0–100 m depth and the upper part of South Atlantic Central Water (SACW) (100–500 m). There is also the Salinity Maximum Water on the boundary of these two water masses, that was formed in the central subtropical gyre (Stramma et al., 2005). General patterns of the western north equatorial circulation, according to (Bruce et al., 1985), include a large anticyclonic eddy (diameter approximately 300–400 km) to the 7–10° N and a southern eddy-like feature (3–6° N). Anticyclonic eddy features exist in the NBC upstream from the retroflection (Johns et al., 1998) and they may propagate downstream within the NBC and serve as a catalyst for NBC ring shedding.

The NBC divides into both surface and subsurface layers of the NECC/NEUC system (Wilson et al., 1994). There are three possible pathways for continuation of the NBC upper part (0–100 m) to the north: the coastal boundary current (Csanady, 1985; Candela et al., 1992), rings from the NBC retroflection (Didden and Schott, 1993; Richardson et al., 1994; Fratantoni et al., 1995; Johns et al., 1998), and offshore retroflection of the current into the NECC (Mayer and Weisberg, 1993). The NECC lies between 3° N and 10° N, roughly considered to be the northern boundary for the SEC (Peterson and Stramma, 1991; Bourlès et al., 1999). Both the NECC and the SEC are the strongest from July to September and are also at their northernmost positions during this time (Peterson and Stramma, 1991). The retroflection of the NBC is considered to be the main source of the NECC (Wilson et al., 1994; Bourlès et al., 1999; Schott et al., 2002), while additional sources for the latter are both the retroflected NEC transport and the northern branch of the SEC (Wilson et al., 1994). The thermocline NBC flow (in the 100–300-m layer) could also feed the NEUC between 2° N and 5° N (Johns et al., 1998). Some of thermocline flow of the NEUC may also recirculate back into the NBC by means of the semipermanent anticyclonic "Amazon" eddy centered near 2° N (Bruce et al., 1985).

Caused by the Atlantic trade wind belt, the NEC is found in the North Atlantic from about 7° N to about 20° N (Schott et al., 2002) and is a broad westward flowing current that forms the southern limb of the North Atlantic subtropical gyre (Bourlès et al., 1999). The Guinea Dome (GD) is a permanent thermal upwelling dome (Rossignol and Meyrueis, 1964) centered at 9° N, 25° W and at 10.5° N, 22° W in boreal summer and winter accordingly (Siedler et al., 1992). The main existence conditions for GD existence is a cyclonic circulation composed of the eastward NECC and NEUC along with the westward NEC (Stramma and Schott, 1999).

According Mittelstaedt (1991), reaching the African coast, the NECC bifurcates and a part of its flow goes northwards, forming the Mauritania Current (MC). The summer — early autumn relaxation of the Northeast Trade winds (Lázaro et al., 2005) along with the NECC strengthening are responsible for fact that the MC roughly reaches the 20° N parallel, just south of Cap Blanc. This process is associated with the cessation of upwelling and the Canary Current (CC) in this place (Mittelstaedt, 1991; Stramma et al., 2008).

3.2 Mid-depth ocean

105 Intermediate waters, namely, Antarctic Intermediate Water (AAIW) and Upper Circumpolar Water (UCPW) cross the equator northward mainly in the Western Atlantic between 500 m and 1200 m depth (Oudot et al., 1999). The vertical minimum of potential temperature (Reid, 1997) and more so the intermediate maximum of silicate concentrations (Oudot et al., 1999) are distinguishing features of UCPW in the equatorial zone. AAIW is carried by several interchanging eastward and westward flowing currents in the equator area (Stramma and Schott, 1999; Brandt et al., 2006). Extended horizontal oxygen minimum

110 zones (OMZs) exist in the eastern tropical Atlantic between 200 and 800 m due to microbial respiration of the excessive organic matter from the nearby North African upwelling area weak water ventilation (Karstensen et al., 2008). Extended horizontal OMZs exist in the eastern tropical Atlantic between 200 and 800 m. The core of the North Atlantic OMZ include SACW and AAIW layers (Stramma et al., 2005). The major pathways to the northern OMZ are subsurface eastward jet currents located south of 10° N: the NICC at 2° N, the NEUC at 4° N, and the northern branch of the NECC at 8–9° N (Stramma et al., 2005;

115 Karstensen et al., 2008; Brandt et al., 2010), while the core of the northern OMZ lies further north. The link between these subsurface jet currents and the OMZ is formed simultaneously by the cyclonic circulation around the GD, a general uplift of the isopycnals within the surface and subsurface levels (Siedler et al., 1992; Lázaro et al., 2005).

3.3 Deep ocean

North Atlantic Deep Water (NADW) is formed in the North Atlantic by convection and mixing and transported southward.

120 NADW penetrates into the Equatorial Atlantic at depths almost similar to the Deep Western Boundary Current (DWBC), and bifurcates into an eastward and southward flow, correspondingly into the open ocean and along the western boundary (Mc-Cartney, 1993). According to Wüst (1935), upper NADW (UNADW) can be recognized by the mid-depth salinity maximum (1500-2000 m deep), while middle NADW (MNADW) at 2000–2500 m deep and 3700 m deep lower NADW (LNADW) are recognized by the oxygen maxima. In the Molinari et al. (1992), waters that had been recently ventilated are described as

125 having had contact with the atmosphere either directly or indirectly by mixing on the time scale of the measurable transient tracer — chlorofluorocarbon (CFC). The maximum of one of the CFCs (F11 — trichlorofluoromethane) represents LNADW (Rhein et al., 1998).

Two cores of recently ventilated (with higher levels of F11) NADW from the northern hemisphere are advected along the boundary and east to the Mid-Atlantic Ridge (MAR) (Molinari et al., 1992). A DWBC shallow core is centered at about 1500

130 m and a deeper one — at about 3500 m. The upper core of high F11 content, limited by the 3.2 and 4.7°C potential temperature isotherms, is typically associated with the deeper core, which is limited by the 1.8 and 2.4°C isotherms. The Ceara Rise blocks the flow of the DWBC waters with potential temperature below 1.8°C to the equator, causing it to recirculate back to the north.

More dense Antarctic Bottom Water (AABW) flows northwars though Atlantic Ocean basins and generally lays underneath NADW at the bottom. The velocity field of AABW (water with $\sigma_4 > 45.90$ kg m^{-3}) is influenced by the overlying DWBC

135 (Rhein et al., 1998). The AABW consists of old deep-water masses (Reid, 1994) with negligible F11 concentrations. According to Rhein et al. (1998), AABW bifurcates at the equator: roughly 30% of the northward AABW flow comes to the Guiana Basin

through the Equatorial Channel at 35° W. The large proportion of AABW turns east to the Romanche Fracture Zone and the Eastern Atlantic with a possibility of recirculation in the Brazil Basin. The sloping topography of Guiana Basin as well as the limitation of AABW upper boundary by the strong eastward flowing NADW cause the fact that the northward directed

140 geostrophic flow of AABW is most pronounced only to the east from the Ceara Rise. Passing the Ceara Rise, AABW flows to the Guiana Basin central part. The high level of F11 (> 0.07 pmol kg$_{-1}$) from LNADW affects the closest to it AABW part — the one nearby the Ceara Rise, thus this AABW branch also experiences a rise in F11 content in comparison with the far eastern AABW branch. To the north from the Ceara Rise similar conditions are found (Rhein et al., 1998). According to (Whitehead Jr and Worthington, 1982; Rhein et al., 1998), the core of AABW is located to the east the Ceara Rise at 43.3° W.

145 AABW mixes with LNADW in the fracture zones at equator, so AABW in the Eastern Atlantic differs from the similar water in the Western Atlantic (Rhein et al., 1998). There are two important features for the Eastern Equatorial Atlantic (McCartney et al., 1991). First, the potential flow of AABW through the Kane Gap from the Sierra Leone Basin to the Gambia Abyssal Plain and back. Second, the potential AABW flow through the Vema Fracture Zone.

According to Arhan et al. (1998) the eastward transport of NADW along the equator is weak, but nevertheless plays a

150 leading role for the maintenance of the equatorial tongue of UNADW. Even though the eastward mean velocities are weak in the equatorial tongues of NADW, the question is of the ultimate fate of this flow as it reaches the African continental slope. There are two cyclonic flows in the deep layers of Eastern Atlantic, associated with NADW — the Gambia Basin one and the Sierra Leone Basin.

4 Results and discussion

155 ### 4.1 SPM concentration

The distribution of SPM within the Ioffe-2000 transect is presented in Figure 3, while background hydrophysical and hydrochemical conditions were described in detail in (Sarafanov et al., 2007). The obtained volume SPM concentrations varied from 0.01 to 0.40 ppm within the Ioffe-2000 transect and up to 4.1 ppm at the stations at the Northwest African upwelling area.

4.1.1 Upper ocean

160 In the upper layers, most commonly, the vertical distribution of SPM has a surface maximum caused by primary production, decreasing exponentially towards the deep. The main reason for this is the fact that the upper ocean contain both the external SPM sources (river discharge, atmospheric input) and the internal SPM sources (primary production) (Chester, 1990). Another reason for particle accumulation in the surface layer may be the pycnocline, which slows the sedimentation (Emelyanov, 2005). The "sedimentation barrier" was presented by a visible pycnocline at depths of 50–150 m to the west of the 30° W and 0–100

165 m to the east of this point on the Ioffe-2000 transect (Sarafanov et al., 2007). It was shown for the Eastern Equatorial Atlantic that the largest particulate elemental and mass concentration gradient occurs at the base of the mixed layer, where the particle and organism maximums are located. The vast majority of particles in the upper open ocean waters is internal and is consists
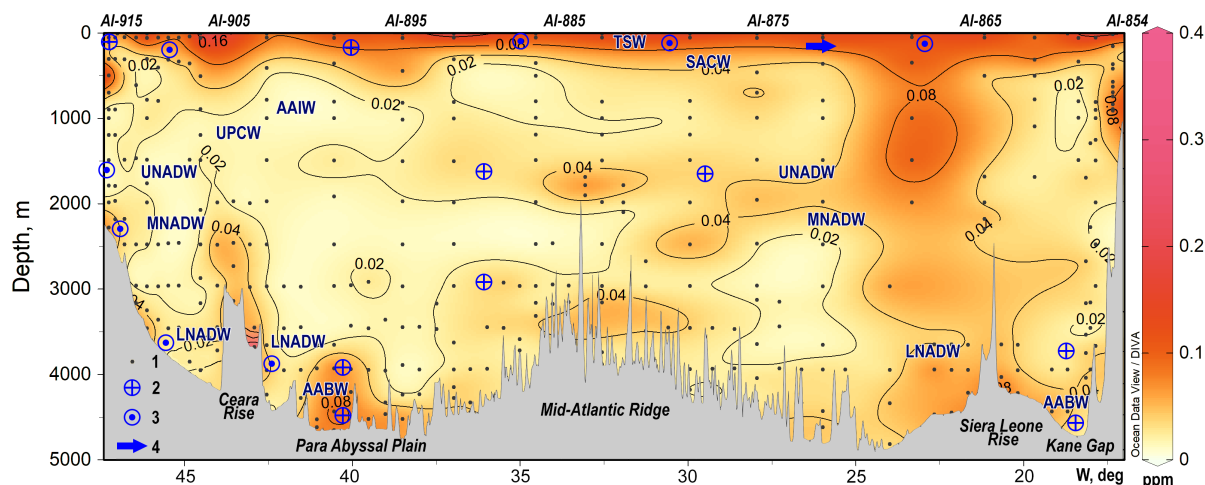
Figure 3. Distribution of the SPM volume concentration (ppm) on the Ioffe-2000 transect, done with (Schlitzer, 2018). 1 — sampling points, 2 — northward current, 3 — southward current, 4 — eastward current. Isolines are in geometric progression, water masses abbreviations see in text. Bottom topography from Sokov et al. (2002)

basically of particulate organic matter (POM), $CaCO_3$, and biogenic silica. A large proportion of the POM produced in surface waters is regenerated in the euphotic zone. Although the net transport of organic matter have to be downward to fuel the lower

170 layers of the water column, there is also an upward component to transport. Positively buoyant particles, including lipid-rich eggs, larvae and, possibly, carcasses of deep-sea animals are examples of particles which undergo upward transport (Smith et al., 1989).

The Ioffe-2000 transect did not reach the SPM-rich coastal waters, yet the coastal SPM source has caused local SPM maximum at the margins of the transect at a depth of 400–800 m (up to 0.18 ppm). It was the Amazon River that caused the

175 far more pronounced influence of the American coast in comparison with the African one. It is well known that the surface SPM transport from the Amazon River to the open ocean turns to the north-east alongside the coast (Gibbs, 1974). According to Sarafanov et al. (2007), the warm, high-saline and silicate-poor upper waters observed on the Ioffe-2000 transect above 400–500 m were advected mostly by the NBC. The NBC core was located immediately westward of the studied transect near the shelf break (Johns et al., 1998). A signature of the NBC eastern periphery is located between 46° W and 47° W at depths

180 of 150–500 m (Sarafanov et al., 2007). The SMP concentrations within the NBC are relatively low. The main evidence of the SPM supply from the Amazon River to the shelf and the continental slope is a huge sediment body — the Amazon Cone. Bottom SPM maxima of Amazon River origin are able to form INL falling from the shelf break. INLs are mostly caused by the detachment of BNLs over the breaks in the slope (McCave et al., 2001). One of the INLs was apparently observed during the Ioffe-2000 transect as a significant rise in the SPM concentration below the NBC.

185   Sarafanov et al. (2007) shows the NEUC equatorward pathway at 44–46° W. We have suggested that such V-shaped isopy-
cnals at 46° W between the NBC and NEUC (Sarafanov et al., 2007, Fig. 3A) correspond with the aforementioned large
eddy-like feature, the semi-permanent "Amazon Eddy" (Bruce et al., 1985).

The northern branch of the SEC (nSEC) is associated with the northwestward or northward near-surface flow at 38–41° W,
which recirculates northward into the NECC. Probably, the local surface maximum of the SPM concentration at 44° W was
190   caused by the nSEC and NECC convergence. The surface SPM maximum was also noted in the most intense cross-transectal
flow of the NECC at 35–37° W (Sarafanov et al., 2007).

The eastward rise of the isopycnals at 28–25° W and their deepening at 24.5–21.5° W at 150–500 m indicate the southern
periphery of the GD on the Ioffe-2000 transect (Sarafanov et al., 2007, Fig 3(a)). Immediately east of the GD (21.5–18° W)
the S-shaped double rotation (a combination of the cyclonic and anticyclonic structures) of the NEUC (Stramma et al., 2008,
195   fig. 12) occered. It is known that the GD influences biological activities, so the chlorophyll-a concentration is high in this
region and linked to the intensity of the doming (Signorini et al., 1999; Pradhan et al., 2006; Doi et al., 2009). So the local
SPM maximum in the GD area within the Ioffe-2000 transect correlate with this data. Overall, the SPM distribution within the
Ioffe-2000 transect's upper layer mainly reflects surface circulation patterns (Biscaye and Eittreim, 1977) as well as particle
transport (vertical and horizontal).

200   **4.1.2   Mid-depth ocean**

According to Sarafanov et al. (2007), the intermediate waters on the Ioffe-2000 transect were recorded as an area of low
in salininty and rich in silicate waters, which extends at depths of 400–1200 m. The AAIW main entrance to the Northern
Hemisphere is located in the western part of the transect (west of 36° W). Both AAIW and UCPW do not come along the
Brazilian slope while flowing from the western equatorial basin to the tropical North Atlantic, but rather flow in the interior
205   ocean.

Usually the intermediate waters correspond with the upper part of the clear water minimum. Clear water is referred to the
minimum in the SPM concentration that is commonly located at varyious mid-depths (Biscaye and Eittreim, 1977). Concen-
trations of the SPM within this layer are 10–100 times lower than in the upper ocean but still reflect, in general, a similar
geographic distribution with high values in the coastal zone and the lowest values at the open ocean. As was mentioned above,
210   the clear water layer SPM concentration reflect, also, the lateral supply of the SPM from the coastal areas (Biscaye and Eittreim,
1977). However, the intermediate waters on the Ioffe-2000 transect were not influenced by the lateral source too strongly, so
the SPM concentrations were low (0.01–0.03 ppm).

On the contrary, the wide area below the GD (19–25° W) is noteworthy due to extremely high for this clear water layer SPM
concentration, which primarily reflects the pattern of productivity in the upper waters (Eittreim et al., 1976). We suggest that
215   this SPM-rich area was caused by the extra high bioproductivity levels within the Northwest African upwelling and, probably,
the GD area (Fig. 4). Equatorward transport of the POM is carried out by the interaction of the CC and the aforementioned
system of equatorial currents. Additional explanation for the POM supply is the low dissolved oxygen levels (OMZ signature),

that was observed at 300 to 700 m depth about 20–25° W and further westward to the MAR (Sokov et al., 2002). Not only is the oxygen minimum caused by the POM supply, but it also prevents organic particles from destruction.

4.1.3 Deep ocean

It is known that the vertical and zonal structure of the deep and bottom waters, i.e. NADW and AABW, in the Eastern Atlantic are significantly more homogeneous than in the Western Atlantic. The Eastern Atlantic generally shows low turbidity (SPM concentration) levels within the NADW and AABW in comparison with the Western Atlantic (Eittreim et al., 1976). The water exchange in the deep layers of Eastern Atlantic is almost negligible in comparison with the intense northward flow of AABW to the east of the Ceara Rise in the western basin, that was noted during the Ioffe-2000 transect (Sarafanov et al., 2007).

The Eastern Atlantic. The research to the east of MAR at the Ioffe-2000 transect allowed us to note two peculiarities. The first one was the northward NADW flow through the Kane Gap into the Gambia Basin, while the second one pointed out the dominance of LNADW in the near-bottom layer west of the Sierra Leone Rise.

The deep waters correspond with the lower part of the clear water minimum. However, the abnormally high for these depths SPM concentrations were noted above the Sierra Leone Rise. This SPM concentration anomaly was connected with another one above in the mid-depth ocean. There are also slight horizontal "tail" with increased SPM concentration spreading almost to the MAR. The probable reason for "tail" existence is the cyclonic flow Gambia Abyssal Plain (Arhan et al., 1998). We propose to explain this "vertical anomaly" by using the ballast hypothesis (Armstrong et al., 2001; Louis et al., 2017), which is based on the correlation between the fluxes of particulate organic carbon (POC) and minerals in the deep ocean. Accordinc to hypothesis description in Van der Jagt et al. (2018), biogenic aggregates are ballasted with biogenic and lithogenic minerals, so their sinking velocities increase. Minerals start to get attached to aggregates both in the surface layer and deeper: during the aggregates formation or when aggregates "scavenge" mineral particles while sinking. The fact that ballasted aggregates sink with higher speed is the main reason for them to be remineralized at a greater depth in comparison with non-ballasted aggregates. Differect aggregates are incorporated with different number of minerals due to different stickiness, which is controlled by the amount of transparent exopolymer particles (TEP) (Alldredge et al., 1993). TEP-precursors are produced mainly by phytoplankton (Passow and Alldredge, 1994). The amount of TEP in the ocean is huge, they occure as "sticky" gels (Passow, 2002), so TEP act as a glue matrix for other solid particles (i.e., detritus), forming larger aggregates ("marine snow") and playing a crucial role in the carbon export from the surface to the deep ocean (Passow et al., 2001).

The SPM in regions with high external supply(for example, the North Atlantic) with their high dust sedimentary inputs consists mostly of lithogenic material. For instance, the surface waters off Cap Blanc (Iversen and Ploug, 2010) and GD (Bubnova et al., 2020) are exposed to the Saharan dust. The Saharan dust deposition may cause the abiotic formation of TEP, which results in the aggregates formation and enhancing the POC export (Louis et al., 2017). Dust is able to ballast into marine snow aggregates (and fecal pellets) ans it also increases the oceanic primary production due to input of dust-related micronutrients (Van der Jagt et al., 2018). Potential strength of the so-called "lithogenic carbon pump" (Bressac et al., 2014) potentially depends on the physical and chemical TEP-precursors featured, which, in turn, stand on the composition and physiological state of the phytoplankton community. The Northwest Africa offshore zone shows high levels of primary
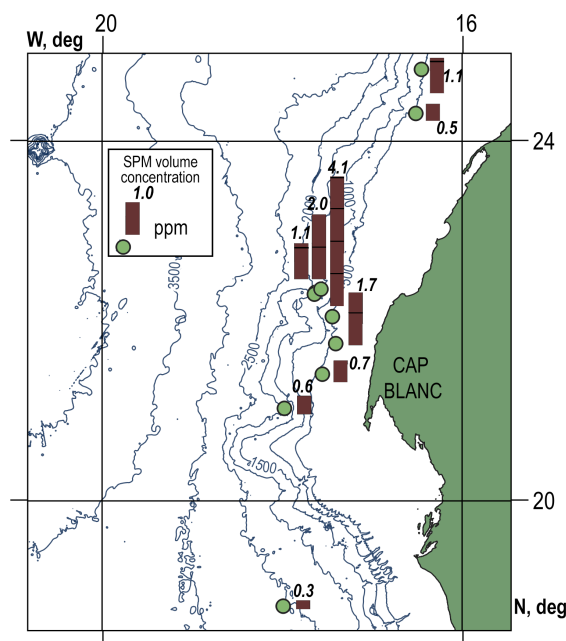
Figure 4. The schematic distribution of surface SPM concentrations (ppm) at the Nortwest Africa upwelling area prior to the Ioffe-2000 transect. Isobaths every 500 m.

production and SPM concentrations (Fig. 4). This area is also exposed to the Saharan dust abundance. The excessive number of ballasted aggregates is lately transported equatorward via CC and consistent flow of the NEC, NECC and GD (equatorial currents system), reaching the Ioffe-2000 transect area.

255   The Van der Jagt et al. (2018) study showed that the total volume of aggregates increased ten times due to dust deposition, while size-specific sinking velocities of the dust-ballasted aggregates incresed two times. It was also shown that the dust-ballasted aggregates carried only 50 percent of the volumetric POC amount in comparison with non-ballasted aggregates. Thus, the overall POC flux driven by dust deposition may rise up to ten times due to the abundance of aggregates. As we remember, fast sinking aggregates are remineralized deeper leading to an increase in the POC fluxes to the deep sea layers

260   (Van der Jagt et al., 2018), which preserves the high SPM concentrations down to the deep ocean. Such fast sinking ballasted aggregates, which were transported from the Northwest Africa upwelling area, caused the abnormally high SPM concentrations above the Sierra leone Rise within the Ioffe-2000 transect.

The Western Atlantic. The vast area to the west of the MAR within the Ioffe-2000 transect experiences an increase in the SPM concentrations, caused by DWBC. It is well-known that there are two reasons for the bottom currents to maintain high

265   loads of SPM: potential resuspension and, far more importantly, selective deposition. The SPM may be transported far within the BNLs, as was shown for clay minerals (Petschick et al., 1996). The most intense BNLs in the western Atlantic are found
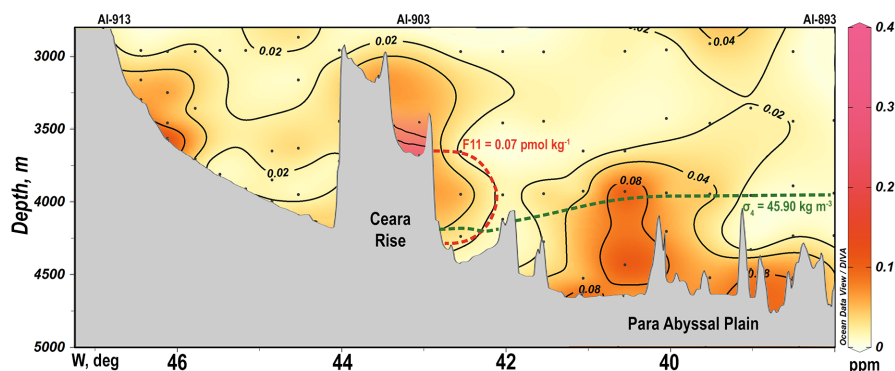
Figure 5. The SPM volume concentration at the western part of the Ioffe-2000 transect: green dashed line — the upper boundary of AABW; red dashed line — the DWBC boundary, based on the F11 (after Rhein et al. (1998), 4.5° N transect). Isolines in geometric progression.

in the southwestern Argentine Basin and northern North American Basin; while the lowest bottom water turbidity is located in the equatorial regions (Eittreim et al., 1976; Biscaye and Eittreim, 1977). Nevertheless, bottom SPM concentrations west of the MAR are still higher in comparison with the eastern part of the Equatorial Atlantic. According to Sarafanov et al. (2007), the

270   southward boundary flow of UNADW was traced in the western basin along the continental slope at the depths of 1400–1500 m. MNADW southward flow was noted at 1900–2600 m with the 100 km wide recirculation. The general LNADW flow was noted at 3700 m depth. The deep cyclonic cell in the Guiana basin (McCartney, 1993; Arhan et al., 1998) at NADW depth near the Ceara Rise western slope and west of the MAR between 42° W and 36–37° W. This northward recirculation of LNADW joins the northward flow of AABW.

275   The noticeable BNL within the western basin is located at 1900–2600 m above the American slope (the Amazon Cone). We suggest that the main reason for its occurence is the interaction between the shallow core of the DWBC and the Amazon River solid load.

    The weak INL deepening from the slope to the east was noted at a depth of 3200–3700 m (Fig. 5). It is enhancing above the Ceara Rise as a result of the DWBC intencification due to the interaction with bottom topography. This INL can be traced to

280   the east from the Ceara Rise (4300 m depthe and 42.5° W), where the deep DWBC core is marked by high F11 level.

    This main reason for the SPM concentration rise at the depth of 3500–4300 m between 41.5° W and 39° W with the peak at 40.5° W is the northward recirculation of SPM-rich LNADW.

    The general northward pathway of AABW ($\sigma_4 > 45.90$ kg m^{-3}) within the Ioffe-2000 transect is located in the Para Abyssal Plain bottom layer. AABW core was found in the 40–42° W troughs, flowing along the Ceara Rise eastern slope (Sarafanov

285   et al., 2007). Studies (Whitehead Jr and Worthington, 1982; Rhein et al., 1998) show AABW core to be separated from the bottom and located at a depth of 4400–4500 m. AABW has high SPM concentrations in comparison with the clear water layer, mostly in the 40–41° W troughs. The SPM concentration maximum within AABW (Fig. 5) is aligned with separated from the bottom AABW core (4400–4500 m). The reason for the separation may be the bottom rise ("dam"), which is located up-stream AABW flow (Whitehead Jr and Worthington, 1982).The "dam" blocks the lower part of AABW flow and coinciding BNL at
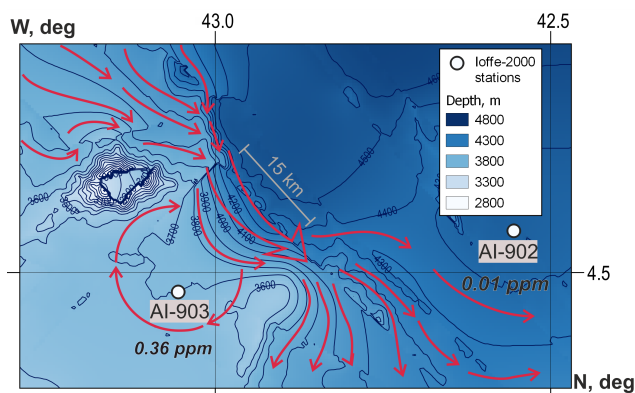
Figure 6. The Ceara Rise SPM maximum: bottom topography (GEBCO Bathymetric Compilation Group, 2020) and the DWBC (red lines).

290   the depth of 4500 m, creatint the INL from BNL. The BNL to the east from AABW flow core is likely caused by AABW
southward recirculation (Sarafanov et al., 2007).

The extremely high SPM concentration (0.36 ppm) was noted in bottom layer above the Ceara Rise (AI-903, depth 3678 m,
18 m.a.b.). The potential reason for that may be interaction between the SPM-rich DWBC and a local feature in the bottom
topography. Figure 6 shows, that AI-903 station was conducted near the terrace brake (3800 m). The terrace slope is low-angle
295   (0.7°), while below the terrace brake lays a far steeper (3.1°) slope (3800–4300 m). This 15-km wide area with the incline drop
perturbs the DWBC core homogenety: the current part above the flat terrace slows down, while the steeper slope suggests a
higher bottom current speed (Bowden, 1960). The current slowing above the terrace is able to cause an eddy. The V-shaped
terrace (see 3700 m isobath) allows to assume that this eddy is the trapped topography one. The eddy originated from the
SPM-rich DWBC causes an additional SPM concentration boost near the bottom. The proposed hypothesis undoubtedly needs
300   to be confirmed by additional research.

The MAR area. High levels of the SPM concentration were also noted above the MAR. The axial region of the MAR
including the rift zone experiences high seismicity and bears a big number of earthquake epicenters as well as the sulfide
mineralization zones of various origins and bedrock zones showing strong hydrothermal imprints (Mazarovich and Sokolov,
2002); in particular in the Sierra Leone fracture zone, i.e. immediately below the Ioffe-2000 transect (see Fig. 1). Both high
305   seismicity and strong hydrothermal activity may be able to cause increased SPM concentrations in the bottom layer. These
factors coincide with tidal currents (Morozov, 2018), potentially causing the INL and BNL above the MAR. The relatively
high SMP concentrations above the MAR may be also caused by the northward recirculation of NADW (Sarafanov et al.,
2007) rich in the SPM, which was noted both sides of the MAR at 36–40° W and 29–32° W.

4.2   Grain-size of the SPM

310   The size distribution of suspended particles is generally considered to be a function of the source and nature of the particles,
processes of aggregation and the "age" of the suspension (McCave, 1985). SPM grain sizes in cumulative number distribution

from Ioffe-2000 transect follow a hyperbolic Junge distribution with slopes between –2.6 and –4.2, which correspond with (McCave, 1975), where slopes were mainly between –2.4 and –3.6. The difference occures due to the fact that (McCave, 1975) had wider size spectum. The overall cumulative number distribution for Ioffe-2000 transect were recorded as a wavy line

315   with an overall slope approximating –3.4 which is similar to (McCave, 1984, 1986; Nowell et al., 1985). The explanation for volume-size distributions was generally based on the results of the HEBBLE project in abyssal waters (the Nova Scotia Rise, 1977–1984) (McCave, 1983; Nowell et al., 1985; McCave, 1985). The sizes measured by a Coulter Counter in this project mainly showed the bimodal structure with a fine mode between 2 and 10 µm and a coarse mode between 20 and 60 µm.

Due to the aperture-tube truncation of 70 µm of the Coulter Counter during the Ioffe-2000 cruise there was a possibility to

320   count the fine part of the coarse mode only. The volume-size distributions display: a) an increased proportion of the 7–21 µm fraction, suggesting the coarse mode, b) a subsidiary fine-mode with the peak size ranges about 2–4 µm, and c) an intermediate mode at 8–13 µm, that was not mentioned in the HEBBLE project.

The most representative volume-size distributions in our study are shown in Figure 7. According to McCave (1983, 1984), there are two most effective physical mechanisms for changing the size distributions: aggregation of small particles (below

325   1.5–8 µm) by Brownian motion and collection of smaller particles by turbulent agitation with larger particles.Thus, the fine mode mainly consists of aggregates. The more turbid suspensions according to (Gardner et al., 1985b) contain a coarser fine mode (∼ 8 µm) than the lower concentration suspensions with a mode of 2–3 µm. According to (McCave, 1984), oceanic particle size volume distribution shows pronounced peaks in BNLs with active resuspension and in surface waters with active primary production. The aggregation rate of 1.5–8 µm particles in the upper ocean depends on filtration by zooplankton. The

330   fine mode, which is weakly pronounced in our data, is explained by a relatively low concentrations (up to 0.36 ppm).

The upper ocean is the area, where the particle production and modification of the initial size distributions occurs most turbulently. Increased shear in pycnoclines and large Brunt-Vaisala frequency generally results in a further smoothing of the size distribution (equivalent to a cumulative particle number distribution with a slope of -3) of SPM (McCave, 1984). The horizontal supply of SPM to the mid-water in the open ocean is relatively slow, therefore, a part of fine material in SPM is

335   old (years old), so the size distribution should not have significant peaks. The flat size distributions are best explained by the sub-equal production of particles of different sized. The coarse mode (20–60 µm), according to McCave (1985), is a result of aggregation, where a significant role is played by mucus. Lately, as was mentioned above in the paper, mucus has started to be referred as TEP. There are no strong vertical gradients of mucus concentration suggesting a bottom source, so it is presumed that the material results from surface productivity and has settled rapidly. This viewpoint is supported in (Emery and Honjo,

340   1979), where the same type of material from surface waters is described and called an "(organic) film". It was shown that the film is most abundant in upwelling areas. The intermediate mode (8–13 µm) was dominant in the surface waters (50 m depth) in the samples with high SPM levels (0.3 ppm). Its occurrence is supposedly caused by high concentration of phytoplankton with cell size less than 10 µm, as well as newborn TEP and detritus. The vertical distribution of different fraction sizes of phytoplankton in the euphotic zone of the Equatorial Atlantic shows that the dominant plankton cell size at the 50 m depth

345   is 3–20 µm (11.5 µm on average) (Herbland et al., 1985). This intermediate mode could not be revealed during the HEBBLE project, because the project was aimed exclusively at abyssal waters.
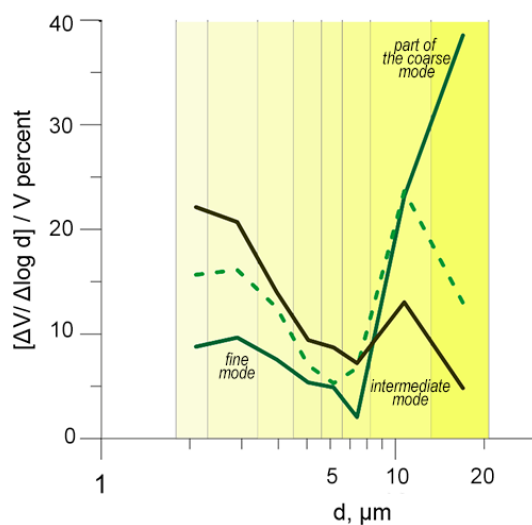
Figure 7. The typical examples of the bimodal volume-size SPM distribution. X-axis is particle diameter, Y-axis is probability density function. Green solid line — dominance of coarse TEP (station AI-898, 3927 m); dashed green line — intermediate mode, caused mostly by phytoplankton, detritus and TEP (station AI-875, 54 m); solid brown line — distribution, potentially caused by the weakened TEP-mode (AI-859, 4732 m). Size intervals are marked with color and thin vertical lines.

5 Conclusions

The Ioffe-2000 transect presented a "screenshot" of volume SPM distribution in the northern part of the Equatorial Atlantic against the background of hydrographic data. Alongside the general agreement with the three-layer model of the ocean SPM

350 distribution, there were some large regional non-uniformities of SPM concentrations and grain size. The international studies of last two decades allowed us to explain those non-uniformities:

1. The most noticeable anomaly is a wide area of high SPM concentrations above the Sierra Leone Rise spreaded from the upper ocean, through the intermediate layer of clear water and down to the ocean bottom. We suggest that this "vertical anomaly" was originated from the Northwest African upwelling area, where the aggregation process exists, since the plankton

355 exposed to the Saharan dust abundance form a big number of ballasted aggregates. The aggregates were lately transported equa-torward via CC and equatorial currents system (including the GD). Our study results agrees with the fact that higher aggregates numbers and higher sinking velocities may increase the carbon export to deep ocean layers. Changes in dust sedimentation may bring about drastic changes in the global ocean due to the boost that nutrients from dust may do for primary production.

2. Deep and bottom waters of the western part of the Equatorial Atlantic show increased levels of the SPM concentrations.

360 The INL deepening from the American slope to the east was noted at the depth of 3200–3700 m. The high SPM concentrations

in the bottom layer above the Ceara Rise is caused by the interaction between the SPM-rich DWBC and a local feature of bottom topography. AABW has incresed SPM concentrations mostly in the 40–41° W troughs. The SPM maximum is located in AABW core (4400–4500 m), separated from the bottom. The explanation for this may be that the bottom rise located up-stream current serves as a "dam", blocking the lower part of AABW flow and coinciding BNL.

365   3. The sizes of suspended particles in the cumulative number distribution follow a hyperbolic Junge distribution with slopes between –2.6 and –4.2; the averaged slope was approximated as –3.4, which fits into the general understanding.

The volume-size distributions displayed two HEBBLE-comparable modes: a fine-mode 2–4 µm and an increased proportion of the 7–21 µm fraction, suggesting the coarse mode (20–60 µm). There was an additional intermediate mode 8–13 µm. It is well known, that the fine mode is mainly represented by aggregates formed from small particles by Brownian motion. The weakly

370 pronounced fine mode could be suggesting a relatively old age of SPM and low concentrations. The coarse particles (7–21 µm) likely represent aggregates with biogenic mucus (TEP), which plays a significant role in particle aggregation. Additional intermediate mode (8–13 µm) is dominant in the SPM-rich surface waters and is presumable the result of phytoplankton growth and the initial TEP formation.

Data availability. The coordinates (Lat, Lon) of the Ioffe-2000 sampling stations, depths of samplings and volume suspended particulate

375 matter concentrations are given in Supplement 1.

Author contributions. Vadim Sivkov: conceptualization, formal analysis, investigation, resources, supervision, funding acquisition; Bubnova Ekaterina: methodology, data curation, visualization, formal analysis. All authors have read and agreed to the published version of the manuscript.

Competing interests. The authors declare no conflict of interest. The funders had no role in the design of the study; in the collection, analyses,

380 or interpretation of data; in the writing of the manuscript, or in the decision to publish the results.

Acknowledgements. The preliminary data processing and surface ocean data interpretation were conducted with financial support of the state assignment of IO RAS (Theme 0128-2021-0012), the data interpretation and conclusions regarding the modern AABW circulation was supported by Russian Science Foundation (project 19-17-00246). The article was finished in kind memory of academician A.P. Lisitsyn (IO RAS) who helped with this research enormously. Marina Ulyanova and Leyla Bashirova contributed with valuable advices and the fruitful

385 discussions.

References

Alldredge, A. L., Passow, U., and Logan, B. E.: The abundance and significance of a class of large, transparent organic particles in the ocean, Deep Sea Research Part I: Oceanographic Research Papers, 40, 1131–1140, https://doi.org/10.1016/0967-0637(93)90129-Q, 1993.

Arhan, M., Mercier, H., Bourles, B., and Gouriou, Y.: Hydrographic sections across the Atlantic at 7°30N and 4°30S, Deep-Sea Research I, 45, 829–872, 1998.

Armstrong, R. A., Lee, C., Hedges, J. I., Honjo, S., and Wakeham, S. G.: A new, mechanistic model for organic carbon fluxes in the ocean based on the quantitative association of POC with ballast minerals, Deep Sea Research Part II: Topical Studies in Oceanography, 49, 219–236, https://doi.org/10.1016/S0967-0645(01)00101-1, 2001.

Biscaye, P. E. and Eittreim, S. L.: Suspended particulate loads and transports in the nepheloid layer of the abyssal Atlantic Ocean, Marine Geology, 23, 155–172, https://doi.org/10.1016/0025-3227(77)90087-1, 1977.

Bischof, B., Mariano, A. J., and Ryan, E. H.: The North Brazil Current, https://oceancurrents.rsmas.miami.edu/atlantic/north-brazil.html/, online; accessed 20-November-2020, 2003.

Bourlès, B., Gouriou, Y., and Chuchla, R.: On the circulation in the upper layer of the western equatorial Atlantic, Journal of Geophysical Research: Oceans, 104, 21 151–21 170, https://doi.org/10.1029/1999JC900058, 1999.

Bowden, K. F.: The dynamics of flow on a submarine ridge, Tellus, 12, 419–426, https://doi.org/10.3402/tellusa.v12i4.9415, 1960.

Brandt, P., Schott, F. A., Provost, C., Kartavtseff, A., Hormann, V., Bourlès, B., and Fischer, J.: Circulation in the central equatorial Atlantic: Mean and intraseasonal to seasonal variability, Geophysical Research Letters, 33, https://doi.org/10.1029/2005GL025498, 2006.

Brandt, P., Hormann, V., Körtzinger, A., Visbeck, M., Krahmann, G., Stramma, L., Lumpkin, R., and Schmid, C.: Changes in the ventilation of the oxygen minimum zone of the tropical North Atlantic, Journal of Physical Oceanography, 40, 1784–1801, https://doi.org/10.1175/2010JPO4301.1, 2010.

Bressac, M., Guieu, C., Doxaran, D., Bourrin, F., Desboeufs, K., Leblond, N., and Ridame, C.: Quantification of the lithogenic carbon pump following a simulated dust-deposition event in large mesocosms, Biogeosciences, 11, 1007–1020, https://doi.org/10.5194/bg-11-1007-2014.hal-00952676, 2014.

Brewer, P. G., Spencer, D. W., Biscaye, P. E., Hanley, A., Sachs, P. L., Smith, C. L., Kadar, S., and Fredericks, J.: The distribution of particulate matter in the Atlantic Ocean, Earth and Planetary Science Letters, 32, 393–402, https://doi.org/10.1016/0012-821X(76)90080-7, 1976.

Bruce, J., Kerling, J., and Beatty III, W.: On the North Brazilian eddy field, Progress in oceanography, 14, 57–63, https://doi.org/10.1016/0079-6611(85)90005-9, 1985.

Bubnova, E., Kapustina, M., Krechik, V., and Sivkov, V.: Suspended Matter Distribution in the Surface Layer of the East Equatorial Atlantic, Oceanology, 60, 228–235, https://doi.org/10.31857/S0030157420010049, 2020.

Candela, J., Beardsley, R. C., and Limeburner, R.: Separation of tidal and subtidal currents in ship-mounted acoustic Doppler current profiler observations, Journal of Geophysical Research: Oceans, 97, 769–788, https://doi.org/10.1029/91JC02569, 1992.

Chester, R.: Particulate material in the oceans, in: Marine Geochemistry, pp. 321–345, Springer, https://doi.org/10.1007/978-94-010-9488-7{_10, 1990.

Craig, H. and Turekian, K.: The GEOSECS program: 1973–1976, Earth and Planetary Science Letters, 32, 217–219, https://doi.org/10.1016/0012-821X(76)90062-5, 1976.

Csanady, G.: "Pycnobathic" currents over the upper continental slope, Journal of physical oceanography, 15, 306–315, https://doi.org/10.1175/1520-0485(1985)015<0306:COTUCS>2.0.CO;2, 1985.

Didden, N. and Schott, F.: Eddies in the North Brazil Current retroflection region observed by Geosat altimetry, Journal of Geophysical Research: Oceans, 98, 20 121–20 131, https://doi.org/10.1029/93JC01184, 1993.

425   Doi, T., Tozuka, T., and Yamagata, T.: Interannual variability of the Guinea Dome and its possible link with the Atlantic Meridional Mode, Climate dynamics, 33, 985–998, https://doi.org/10.1007/s00382-009-0574-z, 2009.

Eittreim, S., Thorndike, E. M., and Sullivan, L.: Turbidity distribution in the Atlantic Ocean, 23, 1115–1127, https://doi.org/10.1016/0011-7471(76)90888-3, 1976.

Emelyanov, E. M.: The barrier zones in the ocean, Springer Science & Business Media, 2005.

430   Emery, K. and Honjo, S.: Surface suspended matter off western Africa: relations of organic matter, skeletal debris and detrital minerals, Sedimentology, 26, 775–794, https://doi.org/10.1111/j.1365-3091.1979.tb00972.x, 1979.

Fratantoni, D. M., Johns, W. E., and Townsend, T. L.: Rings of the North Brazil Current: Their structure and behavior inferred from observations and a numerical simulation, Journal of Geophysical Research: Oceans, 100, 10 633–10 654, https://doi.org/10.1029/95JC00925, 1995.

435   Gardner, W. D., Biscaye, P. E., Zaneveld, J. R. V., and Richardson, M. J.: Calibration and comparison of the LDGO nephelometer and the OSU transmissometer on the Nova Scotian Rise, Marine Geology, 66, 323–344, https://doi.org/10.1016/0025-3227(85)90037-4, 1985a.

Gardner, W. D., Southard, J. B., and Hollister, C. D.: Sedimentation, resuspension and chemistry of particles in the northwest Atlantic, Marine Geology, 65, 199–242, https://doi.org/10.1016/0025-3227(85)90057-X, 1985b.

Gardner, W. D., Richardson, M. J., Mishonov, A. V., and Biscaye, P. E.: Global comparison of benthic nepheloid lay-
440   ers based on 52 years of nephelometer and transmissometer measurements, Progress in Oceanography, 168, 100–111, https://doi.org/10.1016/j.pocean.2018.09.008, 2018.

GEBCO Bathymetric Compilation Group, .: The GEBCO_2020 Grid–a continuous terrain model of the global oceans and land, https://doi.org/10.5285/a29c5465-b138-234d-e053-6c86abc040b9, 2020.

Gibbs, R. J.: The suspended material of the Amazon shelf and tropical Atlantic Ocean, in: Suspended solids in water, pp. 203–210, Springer,
445   https://doi.org/10.1007/978-1-4684-8529-5{_1, 1974.

Herbland, A., Le Bouteiller, A., and Raimbault, P.: Size structure of phytoplankton biomass in the equatorial Atlantic Ocean, Deep Sea Research Part A. Oceanographic Research Papers, 32, 819–836, https://doi.org/10.1016/0198-0149(85)90118-9, 1985.

Iversen, M. H. and Ploug, H.: Ballast minerals and the sinking carbon flux in the ocean: carbon-specific respiration rates and sinking velocity of marine snow aggregates, Biogeosciences, 7, 2613–2624, https://doi.org/10.5194/bg-7-2613-2010, 2010.

450   Jeandel, C., van der Loeff, M. R., Lam, P. J., Roy-Barman, M., Sherrell, R. M., Kretschmer, S., German, C., and Dehairs, F.: What did we learn about ocean particle dynamics in the GEOSECS–JGOFS era?, Progress in Oceanography, 133, 6–16, https://doi.org/10.1016/j.pocean.2014.12.018, 2015.

Johns, W. E., Lee, T., Beardsley, R., Candela, J., Limeburner, R., and Castro, B.: Annual cycle and variability of the North Brazil Current, Journal of Physical Oceanography, 28, 103–128, https://doi.org/10.1175/1520-0485(1998)028<0103:ACAVOT>2.0.CO;2, 1998.

455   Karstensen, J., Stramma, L., and Visbeck, M.: Oxygen minimum zones in the eastern tropical Atlantic and Pacific oceans, Progress in Oceanography, 77, 331–350, https://doi.org/10.1016/j.pocean.2007.05.009, 2008.

Lal, D.: The oceanic microcosm of particles, Science, 198, 997–1009, https://doi.org/10.1126/science.198.4321.997, 1977.

Lázaro, C., Fernandes, M. J., Santos, A. M. P., and Oliveira, P.: Seasonal and interannual variability of surface circulation in the Cape Verde region from 8 years of merged T/P and ERS-2 altimeter data, Remote sensing of environment, 98, 45–62, https://doi.org/10.1016/j.rse.
460   2005.06.005, 2005.

Louis, J., Pedrotti, M. L., Gazeau, F., and Guieu, C.: Experimental evidence of formation of transparent exopolymer particles (TEP) and POC export provoked by dust addition under current and high p CO2 conditions, PloS one, 12, e0171980, https://doi.org/10.1371/journal.pone.0171980, 2017.

Mayer, D. A. and Weisberg, R. H.: A description of COADS surface meteorological fields and the implied Sverdrup transports
465   for the Atlantic Ocean from 30 S to 60 N, Journal of Physical Oceanography, 23, 2201–2221, https://doi.org/10.1175/1520-0485(1993)023<2201:ADOCSM>2.0.CO;2, 1993.

Mazarovich, A. and Sokolov, S. Y.: Hydrothermal fields in the Mid-Atlantic Ridge: Setting and prospects for further discoveries, Russian Journal of Earth Sciences, 4, 2002.

McCartney, M., Bennett, S., and Woodgate-Jones, M.: Eastward flow through the Mid-Atlantic Ridge at 11 N and its in-
470   fluence on the abyss of the eastern basin, Journal of Physical Oceanography, 21, 1089–1121, https://doi.org/10.1175/1520-0485(1991)021<1089:EFTTMA>2.0.CO;2, 1991.

McCartney, M. S.: Crossing of the equator by the deep western boundary current in the western Atlantic Ocean, Journal of physical oceanography, 23, 1953–1974, https://doi.org/10.1175/1520-0485(1993)023<1953:COTEBT>2.0.CO;2, 1993.

McCave, I.: Vertical flux of particles in the ocean, 22, 491–502, https://doi.org/10.1016/0011-7471(75)90022-4, 1975.

475   McCave, I.: Particulate size spectra, behavior, and origin of nepheloid layers over the Nova Scotian continental rise, Journal of Geophysical Research: Oceans, 88, 7647–7666, https://doi.org/10.1029/JC088iC12p07647, 1983.

McCave, I.: Size spectra and aggregation of suspended particles in the deep ocean, Deep Sea Research Part A. Oceanographic Research Papers, 31, 329–352, https://doi.org/10.1016/0198-0149(84)90088-8, 1984.

McCave, I.: Properties of suspended sediment over the HEBBLE area on the Nova Scotian Rise, Marine Geology, 66, 169–188,
480   https://doi.org/10.1016/0025-3227(85)90028-3, 1985.

McCave, I.: Local and global aspects of the bottom nepheloid layers in the world ocean, Netherlands Journal of Sea Research, 20, 167–181, https://doi.org/10.1016/0077-7579(86)90040-2, 1986.

McCave, I., Hall, I. R., Antia, A., Chou, L., Dehairs, F., Lampitt, R., Thomsen, L., Van Weering, T., and Wollast, R.: Distribution, composition and flux of particulate material over the European margin at 47–50 N, Deep Sea Research Part II: Topical Studies in Oceanography, 48,
485   3107–3139, https://doi.org/10.1016/S0967-0645(01)00034-0, 2001.

Mittelstaedt, E.: The ocean boundary along the northwest African coast: Circulation and oceanographic properties at the sea surface, Progress in Oceanography, 26, 307–355, https://doi.org/10.1016/0079-6611(91)90011-A, 1991.

Molinari, R. L., Fine, R. A., and Johns, E.: The deep western boundary current in the tropical North Atlantic Ocean, Deep Sea Research Part A. Oceanographic Research Papers, 39, 1967–1984, https://doi.org/10.1016/0198-0149(92)90008-H, 1992.

490   Morozov, E. G.: Oceanic Internal Tides: Observations, Analysis and Modeling, Cham: Springer International Publishing, https://doi.org/10.1007/978-3-319-73159-9, 2018.

Mullin, J. and Riley, J.: The colorimetric determination of silicate with special reference to sea and natural waters, Analytica chimica acta, 12, 162–176, 1955.

Nowell, A., McCave, I., and Hollister, C.: Contributions of HEBBLE to understanding marine sedimentation, Marine Geology, 66, 397–409,
495   https://doi.org/10.1016/0025-3227(85)90041-6, 1985.

Oudot, C., Ternon, J.-F., Andrié, C., Braga, E. S., and Morin, P.: On the crossing of the equator by intermediate water masses in the western Atlantic Ocean: Identification and pathways of Antarctic Intermediate Water and Upper Circumpolar Water, Journal of Geophysical Research: Oceans, 104, 20 911–20 926, https://doi.org/10.1029/1999JC900123, 1999.

Passow, U.: Transparent exopolymer particles (TEP) in aquatic environments, Progress in oceanography, 55, 287–333, https://doi.org/10.1016/S0079-6611 (02)00138-6, 2002.

Passow, U. and Alldredge, A.: Distribution, size and bacterial colonization of transparent exopolymer particles (TEP) in the ocean, Marine Ecology Progress Series, pp. 185–198, 1994.

Passow, U., Shipe, R., Murray, A., Pak, D., Brzezinski, M., and Alldredge, A.: The origin of transparent exopolymer particles (TEP) and their role in the sedimentation of particulate matter, Continental Shelf Research, 21, 327–346, https://doi.org/10.1016/S0278-4343(00)00101-1, 2001.

Peterson, R. G. and Stramma, L.: Upper-level circulation in the South Atlantic Ocean, Progress in oceanography, 26, 1–73, https://doi.org/10.1016/0079-6611(91)90006-8, 1991.

Petschick, R., Kuhn, G., and Gingele, F.: Clay mineral distribution in surface sediments of the South Atlantic: sources, transport, and relation to oceanography, Marine Geology, 130, 203–229, https://doi.org/10.1016/0025-3227(95)00148-4, 1996.

Pradhan, Y., Lavender, S. J., Hardman-Mountford, N. J., and Aiken, J.: Seasonal and inter-annual variability of chlorophyll-a concentration in the Mauritanian upwelling: Observation of an anomalous event during 1998–1999, Deep Sea Research Part II: Topical Studies in Oceanography, 53, 1548–1559, https://doi.org/10.1016/j.dsr2.2006.05.016, 2006.

Reid, J. L.: On the total geostrophic circulation of the North Atlantic Ocean: Flow patterns, tracers, and transports, Progress in Oceanography, 33, 1–92, https://doi.org/10.1016/0079-6611(89)90001-3, 1994.

Reid, J. L.: On the total geostrophic circulation of the Pacific Ocean: Flow patterns, tracers, and transports, Progress in Oceanography, 39, 263–352, https://doi.org/10.1016/S0079-6611(97)00012-8, 1997.

Rhein, M., Stramma, L., and Krahmann, G.: The spreading of Antarctic bottom water in the tropical Atlantic, Deep Sea Research Part I: Oceanographic Research Papers, 45, 507–527, https://doi.org/10.1016/S0967-0637(97)00030-7, 1998.

Richardson, P., Hufford, G., Limeburner, R., and Brown, W.: North Brazil current retroflection eddies, Journal of Geophysical Research: Oceans, 99, 5081–5093, https://doi.org/10.1029/93JC03486, 1994.

Rossignol, M. and Meyrueis, A.: Campagnes oceanographiques du Gerad-Treca, Cent. Oceanogr. Dakar-Thiaroye, ORSTOM, Dakar, Senegal, 53, 1964.

Sarafanov, A., Sokov, A., and Demidov, A.: Water mass characteristics in the equatorial North Atlantic: A section nominally along 6.5 N, July 2000, Journal of Geophysical Research: Oceans, 112, https://doi.org/10.1029/2007JC004222, 2007.

Schlitzer, R.: Ocean Data View, https://odv.awi.de/, 2018.

Schott, F. A., Brandt, P., Hamann, M., Fischer, J., and Stramma, L.: On the boundary flow off Brazil at 5–10 S and its connection to the interior tropical Atlantic, Geophysical Research Letters, 29, 21–1, https://doi.org/10.1029/2002GL014786, 2002.

Sheldon, R., Prakash, A., and Sutcliffe Jr, W.: The size distribution of particles in the ocean 1, Limnology and oceanography, 17, 327–340, https://doi.org/10.4319/lo.1972.17.3.0327, 1972.

Siedler, G., Zangenberg, N., Onken, R., and Morlière, A.: Seasonal changes in the tropical Atlantic circulation: Observation and simulation of the Guinea Dome, Journal of Geophysical Research: Oceans, 97, 703–715, https://doi.org/10.1029/91JC02501, 1992.

Signorini, S., Murtugudde, R., McClain, C., Christian, J., Picaut, J., and Busalacchi, A.: Biological and physical signatures in the tropical and subtropical Atlantic, Journal of Geophysical Research: Oceans, 104, 18 367–18 382, https://doi.org/10.1029/1999JC900134, 1999.

Sivkov, V., Zhurov, Y., and Demidova, T.: A new data on the distribution of suspended matter in the North Atlantic, in: Proceedings of the XIV School of Marine geology, vol. 2, pp. 172–173, IO RAN, https://doi.org/In Russian, 2001.

Smith, K., Williams, P., and Druffel, E.: Upward fluxes of particulate organic matter in the deep North Pacific, Nature, 337, 724–726, https://doi.org/10.1038/337724a0, 1989.

Sokov, A., Morozov, E., Shapovalov, S., Borodkin, S., and Demidova, T.: Water structure in the equatorial Atlantic on the basis of the year 2000 transatlantic section, Oceanology, 42, 1–6, 2002.

540 Stramma, L. and Schott, F.: The mean flow field of the tropical Atlantic Ocean, Deep Sea Research Part II: Topical Studies in Oceanography, 46, 279–303, https://doi.org/10.1016/S0967-0645(98)00109-X, 1999.

Stramma, L., Rhein, M., Brandt, P., Dengler, M., Böning, C., and Walter, M.: Upper ocean circulation in the western tropical Atlantic in boreal fall 2000, Deep Sea Research Part I: Oceanographic Research Papers, 52, 221–240, https://doi.org/10.1016/j.dsr.2004.07.021, 2005.

Stramma, L., Brandt, P., Schafstall, J., Schott, F., Fischer, J., and Körtzinger, A.: Oxygen minimum zone in the North Atlantic south and east
545 of the Cape Verde Islands, Journal of Geophysical Research: Oceans, 113, https://doi.org/10.1029/2007JC004369, 2008.

Thorpe, S. and White, M.: A deep intermediate nepheloid layer, Deep Sea Research Part A. Oceanographic Research Papers, 35, 1665–1671, https://doi.org/10.1016/0198-0149(88)90109-4, 1988.

Turekian, K. K.: The fate of metals in the oceans, Geochimica et Cosmochimica Acta, 41, 1139–1144, https://doi.org/10.1016/0016-7037(77)90109-0, 1977.

550 Van der Jagt, H., Friese, C., Stuut, J.-B. W., Fischer, G., and Iversen, M. H.: The ballasting effect of Saharan dust deposition on aggregate dynamics and carbon export: Aggregation, settling, and scavenging potential of marine snow, Limnology and Oceanography, 63, 1386–1394, https://doi.org/10.1002/lno.10779, 2018.

Whitehead Jr, J. and Worthington, L.: The flux and mixing rates of Antarctic Bottom Water within the North Atlantic, Journal of Geophysical Research: Oceans, 87, 7903–7924, https://doi.org/10.1029/JC087iC10p07903, 1982.

555 Wilson, W. D., Johns, E., and Molinari, R.: Upper layer circulation in the western tropical North Atlantic Ocean during August 1989, Journal of Geophysical Research: Oceans, 99, 22 513–22 523, https://doi.org/10.1029/94JC02066, 1994.

Wüst, G.: Die Stratosphäre des Atlantischen Ozeans, Deutsche Atlantische Exped, Meteor 1925–1927, Wiss. Erg, 6, 288, 1935.